8-1-1998

Orientational Susceptibility and Elastic Constants Near the Nematic-Isotropic Phase Transition for Trimers with Terminal-Lateral-Lateral-Terminal Connections

Daeseung Kang
Case Western Reserve University

Milind P. Mahajan
Case Western Reserve University

Rolfe G. Petschek
Case Western Reserve University

Charles Rosenblatt
Case Western Reserve University

Chaobin He
University of Southern Mississippi

See next page for additional authors

Orientational susceptibility and elastic constants near the nematic-isotropic phase transition for trimers with terminal-lateral-lateral-terminal connections

Daeseung Kang,[1] Milind P. Mahajan,[1] Rolfe G. Petschek,[1] Charles Rosenblatt,[1] Chaobin He,[2] Puwei Liu,[2] and A. C. Griffin[2,3]

[1]*Department of Physics, Case Western Reserve University, Cleveland, Ohio 44106-7079*

[2]*Department of Chemistry & Biochemistry, University of Southern Mississippi, Hattiesburg, Mississippi 39406*

[3]*Department of Polymer Science, University of Southern Mississippi, Hattiesburg, Mississippi 39406*

(Received 10 February 1998)

Magnetically induced Freedericksz measurements were performed in the nematic liquid crystal phase to extract the elastic constants of a terminal-lateral-lateral-terminal trimer, i.e., a trimer in which the connections to the first and third mesogens are at the end of the mesogen and both attachments to the central mesogen are lateral. Polymeric liquid crystals based on this unit have negative Poisson ratios. Additionally, electric field Kerr measurements were performed in the isotropic phase to extract the orientational susceptibility. The elastic constants were found to be similar to values obtained for typical monomers, albeit with a slightly enhanced ratio K_{33}/K_{11} and reduced ratio K_{11}/K_{22}, especially near the transition temperature. The temperature dependence of the susceptibility was found to deviate significantly from that of typical monomers. The observed behavior is discussed in terms of coupled order parameters representing the terminal and core mesogens of the molecule. [S1063-651X(98)11408-3]

PACS number(s): 61.30.Gd, 64.70.Md

Most polymeric materials exhibit a positive Poisson ratio, i.e., they become thinner when stretched. This is because, under tensile strain, polymers generally develop more order, facilitating interdigitation of groups along the main chain. One can imagine, however, cases where the Poisson ratio is negative, wherein the material exhibits a lateral *expansion* on stretching [1,2]. This behavior has been found in some bulk polymers [2–6] and metal foams [5]. For some of these polymers the negative Poisson ratio—sometimes called ''auxetic''—behavior is based upon atomic scale mechanisms [7,8]; in others, the auxetic behavior is based upon an inverted honeycomb (reentrant cell) molecular structure [1,3,9]. Because of some undesirable physical properties associated with the honeycomb polymers, He, Liu, and Griffin synthesized a new class of auxetic materials based upon site-connectivity-driven rod reorientation in main chain liquid crystalline polymers [10]. The principle of this design concept is illustrated schematically in Fig. 1, wherein alternating mesogens are connected at their ends or cores by flexible spacer groups. In the nematic phase the molecules interact via a combination of anisotropic van der Waals and steric interactions, giving rise to a molecular arrangement in which the mesogenic axes are approximately parallel to each other [Fig. 1(a)]. When stretched, however, the spacer groups become fully extended, causing the core-linked mesogens to orient at a large angle, or even perpendicular, to the main chain direction [Fig. 1(b)]. X-ray results on one such material indeed show increased lateral separation between chains when the polymer fiber is stretched [10].

A low molecular weight trimer has also been synthesized (Fig. 2). The trimeric liquid crystal was prepared by a multistep synthetic route which will be described in a forthcoming paper [11] on trimers and polymers, having the central rod laterally attached to the connecting spacers. This compound was subjected to standard chromatographic and spectroscopic techniques for purity and structure determination. Its phase transition sequence is crystalline-137.9 °C-nematic-154.6 °C-isotropic. The trimer contains two terminal end-connected mesogens and a central core-connected mesogen, and is shown schematically in Figs. 1(c) (ordered nematic) and 1(d) (stretched). Unlike the polymer, the trimer flows easily, with a relatively low viscosity, which is not much different from that of typical low molecular weight nematics. To better understand the nature of the auxetic architecture as it applies to low molecular weight molecules, we examined the elastic constants in the nematic phase and the orientational susceptibility in the isotropic phase above the nematic-isotropic transition temperature T_{NI}. Our central results are that although the splay, twist, and bend elastic constants are not greatly different from those of typical monomers, the pretransitional behavior of the Kerr coefficient in the isotropic phase differs markedly from its monomer counterparts [12].

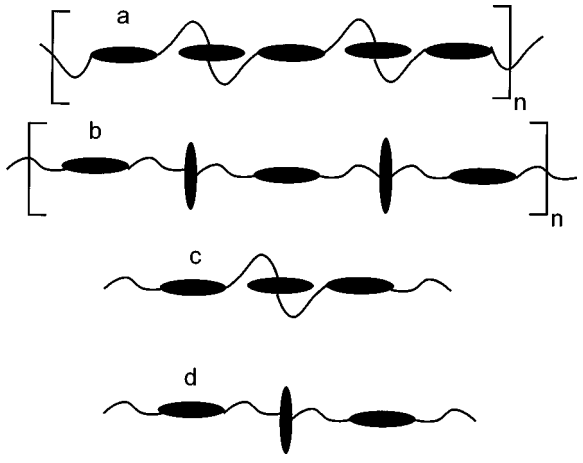

FIG. 1. Schematic representation of auxetic polymer in the nematic phase. (a) Oriented mesogens with significant gauche behavior in the spacer groups. (b) Stretched polymer with elongated spacer groups. (c) Same as (a), except for the trimer. (d) Same as (b), except for the trimer.

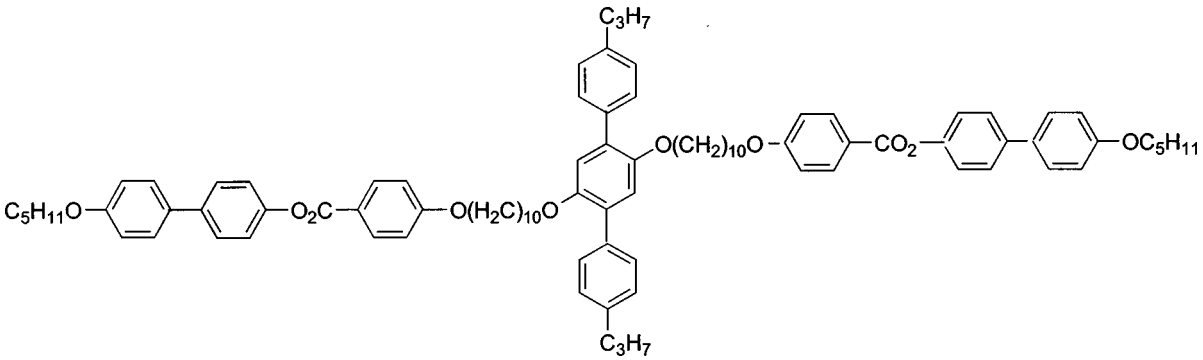

FIG. 2. Chemical structure of the trimer.

To measure the elastic constant, we employed a magnetically induced Freedericksz transition technique, whereby a monodomain liquid crystal cell is subjected to a magnetic field [12]. Above some threshold field $H_{\rm th}=(\pi/d)\sqrt{K_{ii}/\Delta\chi}$ a distortion of the director profile sets in, which can be observed by a change in optical retardation or capacitance of the cell. Here d is the cell spacing; K_{11} is the splay, K_{22} the twist, or K_{33} the bend elastic constant; and $\Delta\chi[\equiv\chi_{\parallel}-\chi_{\perp}]$ is the magnetic susceptibility anisotropy, where $\chi_{\parallel}$ corresponds to the susceptibility parallel to the director $\hat{n}$, and $\chi_{\perp}$ to the susceptibility perpendicular to $\hat{n}$. $\Delta\chi$ was obtained with a Faraday susceptometer. The instrument and technique are described in detail elsewhere [13], and the results for $\Delta\chi$ are shown in Fig. 3. Because of the scatter in $\Delta\chi$, we also measured the optical birefringence Δn in the nematic phase. This measurement was performed at wavelength $\lambda=6328$ Å using a 5-mW He-Ne laser. A planar sample ($d=4.0$ μm) and a Babinet-Soleil compensator were placed between a pair of crossed polarizers, and the compensator was adjusted to achieve a null at the detector. Thus the birefringence was extracted from $\Delta n=\alpha\lambda/2\pi d$, where α is the optical retardation of the Babinet-Soleil compensator; the results are shown in Fig. 4. To a reasonably good approximation we expect that $\Delta\chi\propto\Delta n$. We therefore fitted the birefringence data to an *ad hoc* form: $\Delta n=A(T-T^*)^{\phi}$, where A is a constant and the fitted value of $\phi=0.217$. (We shall see later that the system does not exhibit traditional, single order parameter mean field behavior.) We then overlaid the magnetic susceptibility data in Fig. 3 with this fitted polynomial, adjusting only the amplitude to give a best fit to the $\Delta\chi$ vs T data. Points along this fitted curve were used in the analysis of the threshold field $H_{\rm th}$ in order to determine K_{ii}.

To measure the splay elastic constant, two indium-tin-oxide (ITO)-coated slides were spin coated with polyimide PI2555 (DuPont) and buffed unidirectionally to facilitate planar alignment of the liquid crystal. The cells were separated by Mylar spacers and cemented; the thickness was determined with a micrometer to be (23 ± 1) μm. The cell was then placed into an oven temperature controlled to 0.1 °C, which in turn was placed between the poles of an electromagnet; the magnetic field $\vec{H}$ was oriented perpendicular to the cell. An Andeen-Hagerling model 2500A capacitance bridge operating at 1 kHz was used to measure the cell capacitance *in situ*. The magnetic field was slowly stepped up from zero to 8000 G over 300 s, and the capacitance was computer recorded. A well-defined threshold was observed in the capacitance at $H_{\rm th}$, and, assuming rigid anchoring at the cell walls, K_{11} was extracted from $K_{11}=H_{\rm th}^2 d^2\Delta\chi/\pi^2$. The results are shown in Fig. 5.

The twist elastic constant K_{22} was determined optically. A pair of microscope slides was treated as above for planar alignment; the thickness was determined to be $d=(23\pm1)$ μm. The cell was inserted into the magnet with $\vec{H}$ parallel to the cell and perpendicular to $\hat{n}$. The beam from a 5-mW He-Ne laser passed consecutively through a light chopper, a polarizer oriented at 45° with respect to $\vec{H}$, a focusing lens, the cell (with the beam perpendicular to $\hat{n}$),

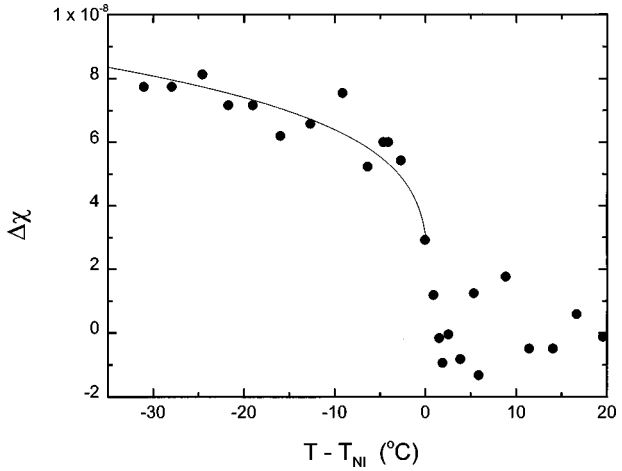

FIG. 3. Magnetic susceptibility anisotropy vs $T-T_{\rm NI}$, where $T_{\rm NI}=165.4$ °C. The solid curve below $T_{\rm NI}$ represents an *ad hoc* fit of the birefringence data (Fig. 4), scaled to overlay the magnetic susceptibility data, and is used for determining the elastic constants.

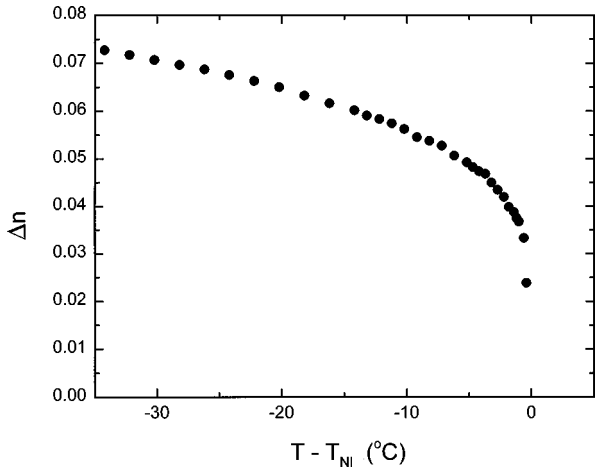

FIG. 4. Optical birefringence vs $T-T_{\rm NI}$ in the nematic phase.

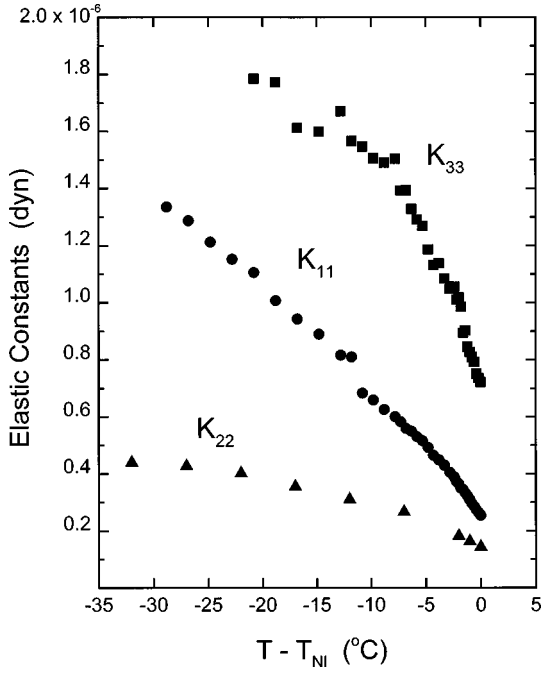

FIG. 5. Splay (K_{11}, ●), twist (K_{22}, ▲), and bend (K_{33}, ■) elastic constants vs $T-T_{\mathrm{NI}}$.

and an analyzer, and into a photodiode detector. The detector output was fed into a lock-in amplifier referenced to the light chopper, and the output from the lock-in amplifier was computer recorded. The magnetic field was again stepped up over 300 s, and the Freedericksz threshold field H_{th} was determined by a sudden increase in the detector signal. For $H > H_{\mathrm{th}}$ a twist distortion was obtained. For thick cells and large optical birefringence the two components of the optical polarization would ordinarily follow the director, emerging from the sample with the same orientation and retardation as in the absence of twist distortion [12]. Fortunately the optical birefringence and the cell thickness were sufficiently small to obviate this situation, resulting in a clear change in the optical signature at H_{th}. Again assuming rigid anchoring conditions, the twist elastic constant is $K_{22}=H_{\mathrm{th}}^2 d^2 \Delta\chi/\pi^2$. K_{22} is shown in Fig. 5.

To measure the bend elastic constant, one ordinarily uses a Freedericksz transition technique in the homeotropic geometry. Although we tried numerous surfactants and polyimides to achieve homeotropic alignment, we were unsuccessful. Instead we used a twisted planar cell, where the director orientation at one surface was rotated by 90° with respect to the other surface, giving a uniform twist throughout the cell. For this geometry the threshold field $H_{\mathrm{th}}=(2/d\sqrt{\Delta\chi})((\pi^2 K_{11}/4)+[\pi^2(K_{33}-3K_{22})/16])^{1/2}$ [14]. Therefore, from measurements of K_{11} and K_{22}, as well as H_{th}, we were able to extract the bend elastic constant K_{33}. ITO slides were used, and the surfaces were prepared as before; the cell spacing was (24.5 ± 1) μm. The cell was placed into the magnet with $\vec{H}$ perpendicular to the cell surface, and the field was again ramped up over 300 s. H_{th} was determined from measurements of the capacitance vs H, from which K_{33} was extracted and shown in Fig. 5.

We also examined the orientational susceptibility in the isotropic phase using an electric-field-induced birefringence (Kerr) technique. A pair of clean but otherwise untreated ITO-coated glass slides was separated by Mylar spacers and cemented together; the cell thickness was (5 ± 1) μm. The beam from a 5-mW He-Ne laser passed consecutively through a light chopper, a polarizer, a Babinet-Soleil compensator, a focusing lens, the sample, and an analyzer, and into a detector. In order to detect the electrically induced optical phase shift α through the sample, the cell was rotated by an angle of 45° about an axis perpendicular to the beam.

Owing to the very small magnitude of the induced phase shifts ($\alpha<10^{-4}$), a phase sensitive detection scheme was used to measure the susceptibility [15]. The detector intensity I is given by $I=I_o\sin^2\alpha$, where I_o is the maximum intensity, $\alpha=\alpha_{\mathrm{cell}}+\alpha_{\mathrm{comp}}$, and α_{comp} is the optical phase shift of the compensator. The phase shift associated with the cell is $\alpha_{\mathrm{cell}}=k(n_e^{\mathrm{eff}}d_e-n_o d_o)$, where k is the wave vector of light ($k=9.93\times10^4$ cm^{-1}), n_e^{eff} is the effective extraordinary refractive index, n_o is the ordinary refractive index, and d_e and d_o the optical pathlengths through the cell for extraordinary and ordinary light, respectively. As usual, $n_e^{\mathrm{eff}}=(\cos^2\varphi_e/n_o^2+\sin^2\varphi_e/n_e^2)^{-1/2}$, where φ_e, the extraordinary angle of refraction inside the tilted cell, is determined implicitly from Snell's law, viz., $\sin\varphi_i=n_e^{\mathrm{eff}}\sin\varphi_e$. The ordinary refractive angle φ_o in the cell is likewise obtained from $\sin\varphi_i=n_o\sin\varphi_o$, and the pathlengths are given by $d_o=d/\cos\varphi_o$ and $d_e=d/\cos\varphi_e$. Finally, we have the usual relationship that $\frac{1}{3}n_e^2+\frac{2}{3}n_o^2=n_{\mathrm{iso}}^2$, where the isotropic refractive index n_{iso} was estimated to be the very typical value 1.6 [12]. From this set of seven equations we uniquely obtain the birefringence $\Delta n=n_e-n_o$ from a measurement of α_{cell}, where $\Delta n\propto\alpha_{\mathrm{cell}}$ for small phase shifts. We thereby can extract the quantity $d\Delta n/dE^2$, which is proportional to the orientational susceptibility dS/dE^2, since $\Delta n\propto S$ for small S.

The sample was driven with an electric field at frequency $f=219$ Hz. For a fixed α_{comp} the intensity for small α_{cell} is given by $I=I_o\sin^2\alpha_{\mathrm{comp}}+I_o\alpha_{\mathrm{cell}}\sin 2\alpha_{\mathrm{comp}}+O(\alpha_{\mathrm{cell}}^2)$, where α_{comp} was chosen to be 0.31 rad and I_o was calibrated by measuring the change in detector output voltage for a given change in α_{comp}. A measurement of I thus yields α_{cell}, which in turn is proportional to Δn. The signal from the detector was input to a lock-in amplifier, which was referenced in the $2f$ mode to the driving voltage. The field was ramped up from 0 to 200 statvolt cm^{-1} over 60 s, and the signal I was recorded. As expected, I was found to be linear in E^2. The magnitude of the susceptibility was obtained from the slope of a linear least squares fit of I vs E^2, and this quantity yields $d\Delta n/dE^2$, whose inverse is plotted against temperature in Fig. 6.

The shape of the inverse susceptibility curve is considerably different from typical electric Kerr or magnetic Cotton-Mouton results above T_{NI} [12], although the magnitude is comparable to other Kerr results [15]. For nearly all low molecular weight materials, the quantities $[d\Delta n/dE^2]^{-1}$ and $[d\Delta n/dH^2]^{-1}$ are linear with temperature over a very wide temperature range. At high temperatures the inverse susceptibility may begin to deviate from linearity, most likely due to conformational changes in the molecule. Close to the transition one often observes a slight concave downward structure to the inverse susceptibility vs temperature [16], often attributed to correlation effects near the nematic-isotropic phase transition. Both the high and low temperature effects

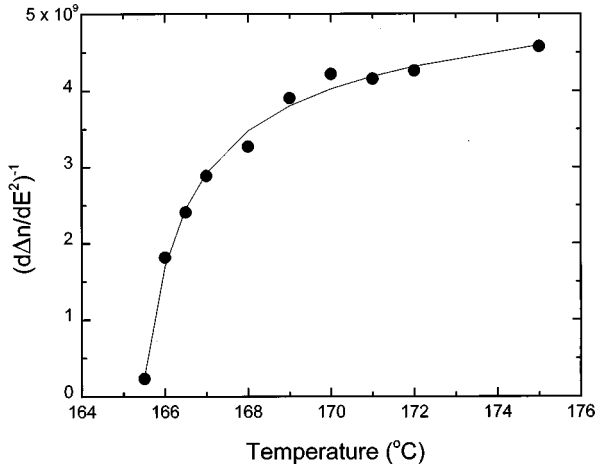

FIG. 6. Inverse order parameter susceptibility vs temperature.

for monomers tend to be modest, however, and for all practical purposes the shape of the inverse susceptibility vs temperature curve is nearly linear. The data in Fig. 6 are clearly different. The concave downward behavior is far stronger than found with other materials. This is especially true close to the transition, where the apparent behavior seems to be much more weakly first order than that of typical low molecular weight nematogens. On fitting the data to the form $d\Delta n/dE^2=\chi_o(T-T^*)^{-\gamma}$, we obtained a not-very-good fit, with an exponent $\gamma=0.35$; this is considerably smaller than the mean field and tricritical values $\gamma=1$. It is smaller still than the $d=3$, $N=5$ n-vector model exponent $\gamma\approx1.53$ [17] associated with the symmetry of the nematic order parameter, the sort of behavior that might be expected for a nearly second order transition [18] close to the transition temperature. As we do not expect crossover critical behavior for this system, we are hard pressed to believe that such a small apparent susceptibility exponent represents true critical behavior of the system.

Instead, we present another, somewhat speculative, explanation. The trimer is composed of three mesogens, where the center mesogen is attached to the spacer groups at its core rather than at its ends. Clearly the environment ''felt'' by the center mesogen is different from the two terminal mesogens, and this must be reflected in the free energy of the system. Moreover, because the mesogens are tethered, macroscopic phase separation is not possible, which places a constraint on the system. If we suppose that S_1 corresponds to the order parameter of the two end mesogens and S_2 to the order parameter of the central mesogen, we can write the most general phenomenological Landau free energy for scalar order parameters as

$$F=aS_1^2+bS_1S_2+cS_2^2-e_1S_1-e_2S_2, \tag{1}$$

where a, b, and c may each have a unique temperature dependence, viz., $a=a_o(T-T_a)$, $b=b_o(T-T_b)$, and $c=c_o(T-T_c)$. The coefficients a_0, b_0, and c_0 are constants, and e_1 and e_2 correspond to $\Delta\chi_1E^2$ and $1/2\Delta\chi_2E^2$, respectively. The model assumes that the effects of the spacer groups can be incorporated into the individual order parameters and coefficients. We note that the cross term bS_1S_2 includes the effects of not only the usual mean field, but the spacer conformations as well. For both S_1 and S_2 to be positive in the nematic phase requires several gauche bonds in the spacer (see Fig. 1). On the other hand, if $S_1>0$ and $S_2<0$, there would be an energetic cost associated with van der Waals interactions and packing, but an energetic advantage associated with an extension of the spacers. On minimizing F with respect to S_1 and S_2, we find

$$S_1=\frac{2ce_1-be_2}{4ac-b^2} \quad \text{and} \quad S_2=\frac{2ae_2-be_1}{4ac-b^2}.$$

We can also write each of S_1 and S_2 as the sum of two partial fractions:

$$S_1=\frac{q_{11}}{T-T_{11}}+\frac{q_{12}}{T-T_{12}}$$

and

$$S_2=\frac{q_{21}}{T-T_{21}}+\frac{q_{22}}{T-T_{22}},$$

where q_{ij} and T_{ij} are constants. After some algebra we find

$$T_{11}=T_{21}=\frac{(2a_oc_oT_a+2a_oc_oT_c-b_o^2T_b)+[(-2a_oc_oT_a-2a_oc_oT_c+b_o^2T_b)^2-(4a_oc_oT_aT_c-b_o^2T_b^2)(4a_oc_o-b_o^2)]^{1/2}}{(4a_oc_o-b_o^2)}$$

and

$$T_{12}=T_{22}=\frac{4a_oc_oT_aT_c-b_o^2T_b^2}{T_{11}(4a_oc_o-b_o^2)}.$$

As the birefringence $\Delta n=\kappa_1S_1+\kappa_2S_2$, where κ_1 and κ_2 are constants that reflect the relative optical weights of the mesogens, we find that the inverse susceptibility is

$$\frac{dE^2}{d\Delta n}=E^2\left[\frac{\kappa_1q_{11}+\kappa_2q_{21}}{T-T_{11}}+\frac{\kappa_1q_{12}+\kappa_2q_{22}}{T-T_{12}}\right]^{-1}. \tag{2}$$

The data may be well fitted to this form, as seen in Fig. 6, where $\kappa_1q_{11}+\kappa_2q_{21}=1.3\times10^{-8}$, $\kappa_1q_{12}+\kappa_2q_{22}=1.9\times10^{-10}$, $T_{11}=110.0\,^\circ$C, and $T_{12}=165.4\,^\circ$C. It is important to recognize that with a four-parameter fit, the χ^2 surface has many shallow minima, and the parameters T_{11} and $\kappa_1q_{11}+\kappa_2q_{21}$ are extremely sensitive to small variations in the data. For example, one of several other comparably good fits may be obtained with the parameters $\kappa_1q_{11}+\kappa_2q_{21}=2.6\times10^{-8}$, $\kappa_1q_{12}+\kappa_2q_{22}=2.1\times10^{-10}$, $T_{11}=40.0\,^\circ$C, and $T_{12}=165.4\,^\circ$C. Therefore, one should not-

draw strong quantitative conclusions from the particular values determined from the fit. Nevertheless, it does appear that the two mesogenic species feel different environments, and individual (but coupled) order parameters may provide a reasonable explanation for the observed behavior. Thus the strongest conclusions that can be drawn from this interpretation of the data is that two order parameters contribute to the signal with very nearly equal and opposite weights far from the transition. Only near the transition do they become substantially different, where the susceptibility of a particular combination diverges. This is consistent with the molecular structure if the two order parameters correspond to the long axes of the central and terminal rods.

A second feature is the closeness of approach of the data toward T_{12}, which is the effective supercooling temperature of the isotropic phase. Although we are not certain that the lowest temperature data point in Fig. 6 is entirely within the isotropic phase, data were certainly gathered in the isotropic phase within 0.5 °C of T_{12}. [Note that the general conclusions drawn above would not be affected even if this lowest temperature point were discarded; the curvature is still far larger than could be explained with only a single order parameter]. A close approach to the supercooling limit has been theoretically associated with a nearby Landau point and biaxial phase on a temperature–molecular-architecture phase diagram, and has been positively observed for a lyotropic liquid crystal [19], and reported for a thermotropic liquid crystal [20] as well. Just below the continuous isotropic–biaxial-nematic transition (the Landau point), the bend and twist elastic constants should be equal. We find no evidence of this, which may suggest that these materials are not, in fact, too close to the Landau point. An examination of other possible biaxial materials in this class of molecules will be the subject of future investigations.

We remark that the apparent small size of the first order transition—this is defined as the closest approach to the supercooling temperature—is interesting in the context of coupled order parameters. If there are coupled order parameters and there are cubic interactions such as $S_1S_2^2$ and $S_2S_1^2$ between them, then the elimination of the less important order parameter results in a small (or negative) quartic term in the primary order parameter. This is then expected to result in a transition with even *more* first order character, which is contrary to our observations in this material. Similar strongly first order behavior is expected if the system is viewed as being an equilibrium mixture of different conformers, each of which couples differently to the nematic order parameter. This may explain why behavior of this nature is unusual in nematic liquid crystals. However, in this system, it is reasonable to suggest that there are couplings between two (or more) order parameters—say the long axes of the central and terminal mesogens—that are mediated by intramolecular interactions via the conformers and bending of a connecting chain. It is also reasonable that the intermolecular interaction between these order parameters are Meier-Saupe-like, i.e., proportional to the product of the order parameters of each molecule. With these assumptions, the quadratic term in the free energy can have any form, depending on the nature of the intermolecular interactions. The nonlinear terms in the free energy would, as usual, come from the entropy associated with the the rotations of the molecule. However, as a molecule rotates (for any given conformer and therefore for any thermal average of conformers, provided the conformers are not strongly affected by order parameter of the medium), all order parameters, that is to say all second rank tensors, will transform in the same way. It follows that all such order parameters can be related to a single order parameter. This in turn implies that a single second rank tensor order parameter can be assigned to the whole molecule, and all such possible tensors can be deduced from the others. Further, it is possible to view the free energy of a single molecule as a function of *one* of these order parameters. Thus the nonquadratic part of the free energy of such a system is a function of this single order parameter. Analysis of such a free energy does not suggest a strongly first order transition; rather, it suggests a ''normal'' first order transition.

The elastic constant data, on the other hand, are similar to typical monomer results in the nematic phase [12]. The calculated bend constant is perhaps slightly larger than generally observed, and the splay constant slightly smaller, although not unusually so. From these data we can conclude that the elastic properties of the nematic are not too dissimilar from those of most monomers, and it is likely that both S_1 and S_2 are positive in the nematic phase. This conclusion is consistent with the x-ray data reported on an auxetic polymer [10], and is therefore consistent with flexible spacer groups connecting the central mesogen with the two terminal mesogens. Due to the flexibility of the spacers, the central mesogen is then able to align in the nematic mean field dominated by the terminal groups. Deviations of the ratios K_{33}/K_{11} and K_{11}/K_{22} from typical monomer values may come about from the central mesogen, which makes the molecule somewhat bulky in the center. Unfortunately, we are not aware of any theoretical treatment of elastic constants for such a molecule. Moreover, as this molecule is not asymmetric (i.e., wedge shaped, bent, or twisted), one would not expect a decrease in the corresponding (splay, bend, or twist) elastic constants. This is borne out experimentally, as there seems to be no significant experimental evidence of such a decrease.

Auxetic liquid crystals represent a new class of molecules with interesting and potentially useful physical properties. Although the system reported herein exhibits elastic behavior not too dissimilar from typical monomers, one can imagine that shorter spacer groups would substantially inhibit the central group from aligning with the terminal groups. Such behavior would likely have a profound effect on the elastic constant ratios, and may more strongly promote a biaxial nematic phase. Moreover, shorter spacer groups would have an important impact on the coupling term in Eq. (1), and significantly affect the behavior of the susceptibility. These issues will be the subject of future investigations.

This work was supported by the National Science Foundation under Grant Nos. DMR-9502825 and DMR-9420843, by the NSF's Advanced Liquid Crystalline Optical Materials Science and Technology Center under Grant No. DMR-8920147, and by the U.S. Air Force Office of Scientific Research under Contract No. F49620-94-1-0454.

[1] K. E. Evans, I. J. Hutchinson, and S. C. Rogers, Nature (London) **353**, 124 (1991).
[2] R. S. Lakes, Science **235**, 1038 (1988).
[3] L. J. Gibson and M. F. Ashby, *Cellular Solids: Structure and Properties* (Pergamon, Oxford, 1988), pp. 70–82.
[4] K. E. Evans, Endeavour **15**, 170 (1991).
[5] E. A. Friis, R. S. Lakes, and J. B. Park, J. Mater. Sci. **23**, 4406 (1988).
[6] K. L. Alderson and K. E. Evans, Polymer **33**, 4435 (1992).
[7] A. E. H. Love, *A Treaty on the Mathematical Theory of Elasticity*, 4th ed. (Dover, New York, 1944).
[8] D. J. Gunton and G. A. Saunders, J. Mater. Sci. **7**, 1061 (1972).
[9] G. Wei and S. F. Edwards, Comput. Polym. Sci. **2**, 44 (1992).
[10] C. He, P. Liu, and A. C. Griffin, Macromolecules **31**, 3145 (1998).
[11] P. Liu, C. He, C. J. Booth, and A. C. Griffin (unpublished).
[12] See, e.g., S. Chandrasekhar, *Liquid Crystals* (Cambridge University Press, Cambridge, 1992).
[13] G. A. DiLisi, E. M. Terentjev, A. C. Griffin, and C. Rosenblatt, J. Phys. II **3**, 597 (1993).
[14] F. M. Leslie, Mol. Cryst. Liq. Cryst. **12**, 57 (1970).
[15] J.-F. Li, V. Percec, and C. Rosenblatt, Phys. Rev. E **48**, R1 (1993).
[16] T. W. Stinson, J. D. Litster, and N. A. Clark, J. Phys. Colloq. **33**, C-1 (1972).
[17] J. C. LeGuillou and J. Zinn-Justin, J. Phys. (France) Lett. **46**, L-137 (1985).
[18] C. Rosenblatt, Phys. Rev. A **32**, 1115 (1985).
[19] L. J. Yu and A. Saupe, Phys. Rev. Lett. **45**, 1000 (1980).
[20] J.-F. Li, V. Percec, C. Rosenblatt, and O. D. Lavrentovich, Europhys. Lett. **25**, 199 (1994).